



Microstructure and thermal stability of sintered pure tungsten processed by multiple direction compression

Ping LI, Da-zhi SUN, Xue WANG, Ke-min XUE, Rui HUA, Yu-cheng WU

School of Materials Science and Engineering, Hefei University of Technology, Hefei 230009, China

Received 12 December 2015; accepted 31 August 2016

Abstract: Multiple direction compression (MDC) was conducted on sintered pure tungsten (99.9%, mass fraction) with different reductions at 1423 K. The microstructure, microhardness and thermal stability of the MDC-processed samples were studied by X-ray diffraction (XRD), electron backscattered diffraction (EBSD) and differential scanning calorimetry (DSC) compared with those of the initial sintered tungsten. The results show that the dislocation density increases significantly with the reduction of MDC, ranging from $3.08 \times 10^{14} \text{ m}^{-2}$ for the initial sintered tungsten to $8.08 \times 10^{14} \text{ m}^{-2}$ for the tungsten after MDC with the reduction of 50%. The average grain size decreases from 83.8 to 14.7 μm and the microhardness value increases from $\text{HV}_{0.2} 417$ to $\text{HV}_{0.2} 521$. The recrystallization temperature for the tungsten samples processed by MDC is approximately constant at around 1600 K. The MDC of sintered tungsten results in a decrease of grain size concurrent with an increase of uniformly distributed nucleation sites, which leads to the improvement of the thermal stability.

Key words: multiple direction compression (MDC); sintered tungsten; dislocation density; mechanical properties; thermal stability

1 Introduction

Tungsten (W) has extensive applications in extremely challenging operation conditions, such as in the aerospace, electronics, chemical and nuclear industries, owing to its characteristic physical properties, nobler chemical stability and excellent high temperature strength [1]. In addition, tungsten has been considered as one of the most promising candidates for plasma facing materials (PFMs) applied in the controlled thermonuclear reactors (CTR) due to the outstanding comprehensive advantages [2]. However, the applications of pure tungsten metal are heavily limited by the low ductile-to-brittle transition temperature (DBTT, 473–673 K), recrystallization brittleness (CRT, 1473–1673 K) and irradiation brittleness [3,4].

The ultrafine-grained (UFG) or nanocrystalline (NC) tungsten material has characteristics of low DBTT, high strength and toughness, good elevated temperature mechanical performance and enhanced thermal shock resistance [5]. Plastic deformation is an effective technique for grain refinement, material densification, microstructure homogenization and mechanical property

improvement to enhance the performance of W-base materials without changing their chemical composition. However, there are limits in the micro-orientation transformation of dislocation cells and grain refinement for the conventional plastic deformation techniques, such as rolling [6], swaging [7] and extrusion processing [8]. So, the comprehensive properties of W are not improved effectively.

Accordingly, severe plastic deformation (SPD) can achieve exceptional microstructure refinement with small grain size in the range of sub-micrometer and even nanometer and enhance the mechanical performance effectively [9]. Therefore, it provides a powerful method to produce ultrafine-grained or nanocrystalline bulk tungsten material with high level of density [10–13] and give potential to enhance the grain boundary strength and improve the ductility.

As one of the typical SPD techniques, multiple direction compression (MDC) is simply repeated compression, in which the sample is subjected to increments of compression accompanied with sequential changes of loading direction along the three perpendicular axes, as shown in Fig. 1. MDC would be especially attractive for scaling-up of relatively large

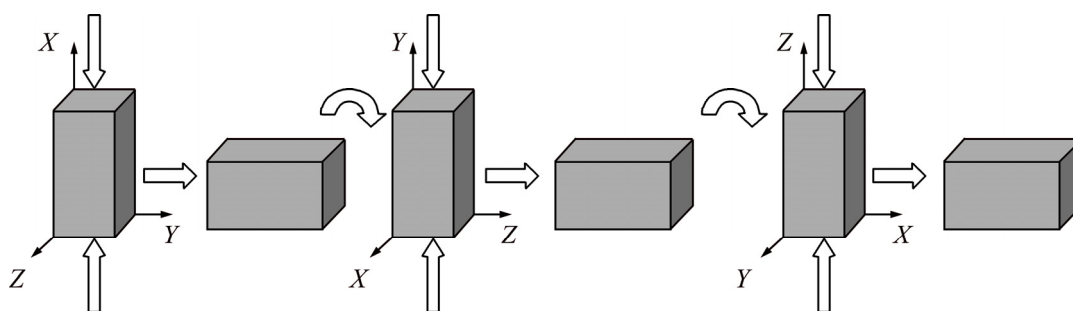


Fig. 1 Schematic diagram of multiple direction compression process

samples using a conventional forging machine without installing any special equipment, which is suitable for industrial applications. Thus, it is expected to fabricate dense bulk refractory materials with refined grains and excellent properties [14,15].

The objectives of this work are to fabricate large-scale bulk tungsten with refined grains and excellent performances by MDC processing, and then to investigate the microstructure evolution, mechanical performance and thermal stability.

2 Experimental

The sintered tungsten rods with a purity of 99.9% and initial relative density of 0.97 were machined to cylinders having the diameter of 16 mm and the height of 15 mm. MDC experiments were carried out on a self-designed 2000 kN pressing and torsion machine (RZU2000HF) with reductions of 30% and 50% at the temperature of 1423 K and ram velocity of 6 mm/s. In addition, the dies were heated to 773 K.

X-ray diffraction (XRD) measurements were performed on the cross section at the center of the samples using a D2500 diffractometer with Cu K_{α} radiation at a scanning step of 0.01° . The parameters of XRD patterns for the tungsten samples were calculated by the software of Jade 6. Dislocation density was calculated from peak broadening analysis of XRD profile lines. The microstructure was characterized further by electron backscattered diffraction (EBSD) using JSM-7001F scanning electron microscope (SEM).

The Vickers microhardness ($HV_{0.2}$) was measured on the cross section at the center of the sample by imposing a load of 2 N for 15 s and 15 separate measurements across the whole sample were taken to evaluate the average microhardness. The thermal stability of the material was investigated by differential scanning calorimetry (DSC) using a STA449F3 analyzer at a constant heating rate of 10 K/min in pure Ar atmosphere with temperature ranging from 273 to 1673 K.

3 Results and discussion

3.1 X-ray diffraction analyses

The analyses based on XRD require the peaks generated by Cu $K_{\alpha 1}$, and hence, the diffraction peaks must be separated by Lorenz function and the $K_{\alpha 2}$ component must be removed in advance. Figure 2 shows the XRD patterns for both the initial sintered tungsten and the MDC-processed samples with different reductions. Based on XRD analyses, the statistical data, diffraction angles (Bragg angle) and peak breadths (integral breadths, IB) on different crystallographic planes, as well as the lattice parameters, are summarized in Table 1. Prior to the XRD analyses, the instrumental peak broadening of the radiation of XRD analyzer was removed and the exact peak positions of the tungsten samples were calibrated by the standard Si powder.

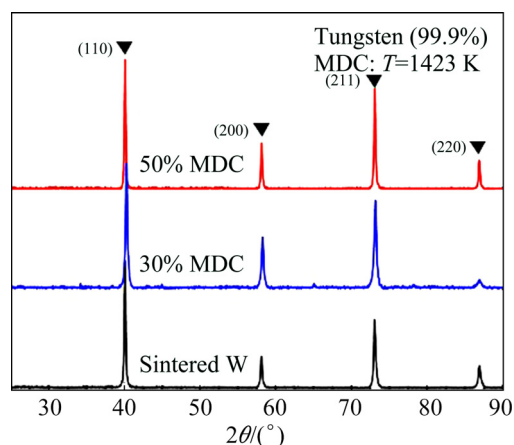


Fig. 2 XRD patterns of tungsten samples with and without MDC processing

According to the curves in Fig. 2 and the data in Table 1, there is apparent peak broadening for the MDC-processed tungsten samples compared with the initial sintered tungsten, which indicates that the plastic deformation imposed by MDC results in the generation of small crystallite size and high level of imperfections in

the deformed sample in the form of lattice distortion and dislocation.

Table 1 Parameters calculated from XRD profiles

Sample	Plane	2θ/(°)	Integral breadth/(°)	a/Å
Sintered W	(110)	40.09	0.2916	3.1696
	(200)	58.14	0.3579	
	(211)	73.05	0.3891	
	(220)	86.92	0.4503	
MDC with reduction of 30%	(110)	40.24	0.3580	3.167
	(200)	58.22	0.4224	
	(211)	73.15	0.4912	
MDC with reduction of 50%	(220)	86.91	0.7014	3.1694
	(110)	40.09	0.4137	
	(200)	58.14	0.5468	
	(211)	73.09	0.6006	
	(220)	86.88	0.7490	

Generally, the broadening of peak breadths for polycrystalline metals is a comprehensive phenomenon resulting from small crystallite size, lattice microstrain and their interactions. A famous mathematic model of Cauchy–Gaussian function, namely Voigt equation, depicts the peak broadening as the following relationship [16–19]:

$$\frac{(\Delta 2\theta)^2}{(\tan \theta)^2} = \frac{K\lambda}{L} \left(\frac{\Delta 2\theta}{\tan \theta \cdot \sin \theta} \right) + 16e^2 \quad (1)$$

where θ equals to the half of Bragg angle; K is Scherrer constant and the value is 0.89 when $\Delta 2\theta$ is selected as the integral breadth (IB) for the metals having cubic crystal lattice; λ is the wavelength of the radiation of XRD analyzer ($\lambda=0.15406$ nm); L is crystallite size with the meaning of an average volume of crystallite dimension which is perpendicular to the reflecting crystallographic plane and has the misorientation angle of 1° – 2° ; e is the lattice strain related to the microstrain $\langle \varepsilon^2 \rangle^{1/2}$ and these two parameters have the following relationship: $e=1.25 \langle \varepsilon^2 \rangle^{1/2}$.

When $\Delta 2\theta/(\tan \theta \cdot \sin \theta)$ is plotted against $(\Delta 2\theta)^2/\tan^2 \theta$, the multi-peak linear fitting results are shown in Fig. 3. The values of crystallite size (L) and microstrain ($\langle \varepsilon^2 \rangle^{1/2}$) can be obtained from the slope and the ordinate intersection from the fitting lines, respectively. For the initial sintered tungsten, the line fitting result shows the average crystallite size of 35.2 nm and a low level of microstrain of about 0.086%. For the sample processed by MDC with the reduction of 30%, the crystallite size has a slight decrease to 33.3 nm and the microstrain increases significantly to 0.153%

compared with the initial sintered tungsten. After the MDC processing with the reduction of 50%, the values of crystallite size and microstrain for the tungsten sample are determined as 28.2 nm and 0.180%, respectively. The data in Fig. 3 indicate a gradual decrease in crystallite size with increasing the strain imposed by MDC processing, whereas the microstrain keeps increasing.

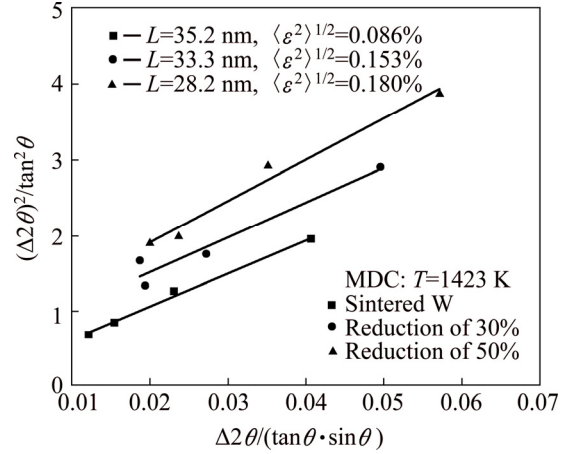


Fig. 3 Voigt plot for tungsten samples with and without MDC processing

Based on the values of crystallite size and microstrain obtained from the Voigt plot, the dislocation density (ρ) can be calculated by using the following equation [20]:

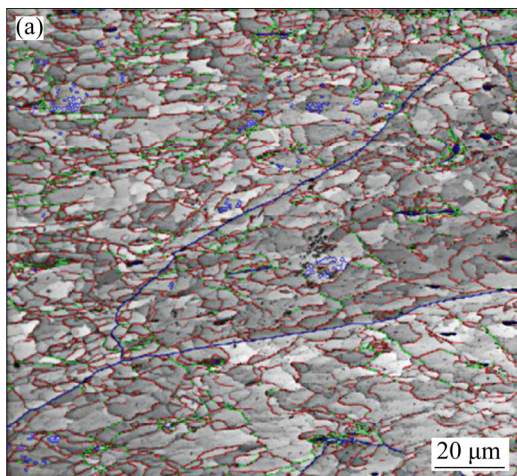
$$\rho = \frac{2\sqrt{3}\langle \varepsilon^2 \rangle^{1/2}}{\|b\|L} \quad (2)$$

where b is Burgers vector with the value related to lattice parameter a (as given in Table 1) in the terms of $\|b\|=\sqrt{3}/2a$ for BCC metals. Therefore, the dislocation density of the initial sintered tungsten is $3.08 \times 10^{14} \text{ m}^{-2}$, and the values experience a significant increase and reach $5.81 \times 10^{14} \text{ m}^{-2}$ and $8.08 \times 10^{14} \text{ m}^{-2}$ for the samples processed by MDC at the conditions of 30% reductions and 50% reductions, respectively, which are about 2–3 times higher than that of the initial sintered tungsten. The results show that the dislocation density in the samples has the positive correlation with increasing the equivalent strain. The induced strain provides more active energy for the atom movement and the generation of a large amount of lattice defects.

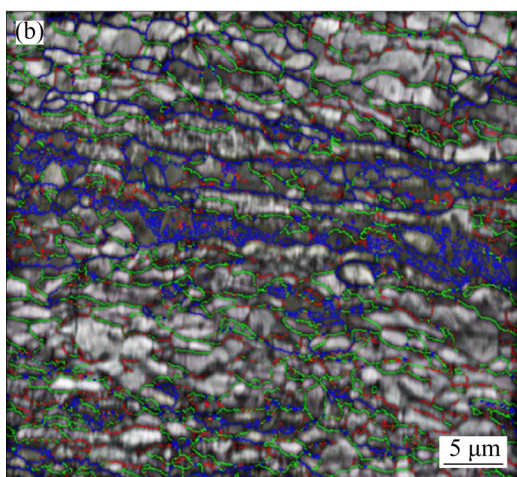
3.2 EBSD analyses

Microstructures of the initial sintered tungsten and the MDC-processed sample with the reduction of 50% obtained by EBSD are shown in Fig. 4. It is apparent that a large number of subgrains with low angle boundaries in the coarse grains interior can be observed in the initial sintered tungsten and the microstructure turns to a mixture consisting of elongated coarse grains and

fine-grain bands after MDC processing. The distributions of grain size with misorientation angle of above 15° and grain boundary misorientation are shown in Fig. 5 and Fig. 6, respectively.



Boundaries: rotation angle			
	Min	Max	Fraction
—	2°	5°	0.669
—	5°	15°	0.211
—	15°	180°	0.120



Boundaries: rotation angle			
	Min	Max	Fraction
—	2°	5°	0.193
—	5°	15°	0.332
—	15°	180°	0.475

Fig. 4 Microstructures of tungsten samples before (a) and after (b) MDC processing with 50% reduction

For the initial sintered tungsten, a few pores can be observed among the coarse grains with the average grain size of about 83.8 μm. The grain size distribution also shows that there is no grains with the size less than 3 μm and nearly all the grains have the size over 37.3 μm. In addition, the histogram for the misorientation angle shows that the average misorientation angle is about 8.5° and the proportion occupied by the grain boundaries with high misorientation angle over 15° is denoted as low as 12.1%.

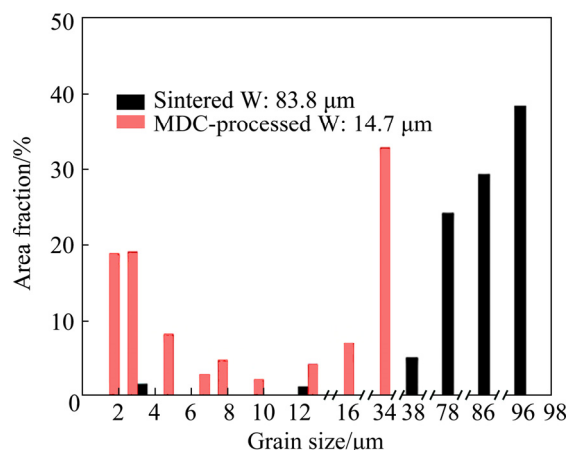


Fig. 5 Distribution of grain size for tungsten samples with and without MDC processing

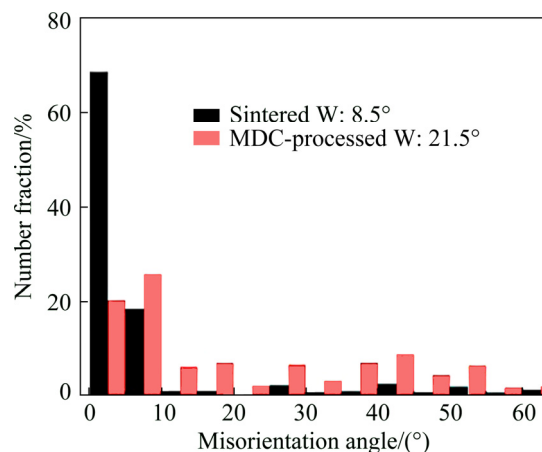


Fig. 6 Variation of misorientation angle for tungsten sample with and without MDC processing

After MDC processing with the reduction of 50%, majority of the pores are closed and fine grains with high-angle grain boundaries are generated. It is found that a significant decrease exists in the value of average grain size to 14.7 μm for the sample processed by MDC. Moreover, the grains with the size less than 3 μm take an overall percentage of 37.9%. The histogram for the misorientation angle demonstrates that the average misorientation angle in the MDC-processed sample reaches 21.5° which is equivalent to an increase of 153% compared with the initial sintered tungsten and the overall percentage taken by the grains with high angle boundaries over 15° experiences an obvious increase to 48.1%.

During MDC deformation, the high levels of dislocations around grain boundaries lead to the generation of subgrains and majority of the subgrain boundaries formed in the grain interior are of low angle [10]. With the deformation proceeding, the subgrain boundaries gradually evolve into high angle grain boundaries through dislocation absorption and the

subgrains transform gradually into equiaxed ones. Therefore, near-equiaxed ultrafine grains separated by straight high angle grain boundaries are generated and the grains are refined greatly.

3.3 Mechanical property analyses

The average Vickers microhardness was introduced to analyze the mechanical property of the MDC-processed tungsten. The microhardness of the initial sintered tungsten is determined to be $HV_{0.2}$ 417 and the value gradually increases from approximately $HV_{0.2}$ 451 with the reduction of 30% to $HV_{0.2}$ 521 with the reduction of 50% after one pass of MDC. According to the principle of MDC processing, the equivalent von Mises strain (ε) imposed on the sample can be calculated as follows [14]:

$$\varepsilon = \frac{\sqrt{3}n}{2} \ln\left(\frac{H}{h}\right) \quad (3)$$

where n is the number of compression; H and h are the height (mm) of the sample before and after MDC processing, respectively.

For the sample MDC-processed with the reduction of 30%, the equivalent strain is about 0.93, and it is as high as 1.8 for the sample MDC-deformed with 50% reduction. The increasing microhardness of the samples may be resulted from grain refinement and strain hardening which are related to the large equivalent strain.

The presence or absence of the cracks around microhardness indentations during the microhardness testing may reflect qualitatively the toughness or ductility of the materials at the testing temperature [21]. The cracks around the microhardness indentations of the tungsten samples are shown in Fig. 7. For the initial sintered tungsten, long branching cracks occur around the indentations, which reveals the brittle essence of the sintered tungsten. As to the tungsten processed by MDC with the reduction of 30%, only a few shorter cracks are observed. Almost no clear cracks are found around the indentations on the sample processed by MDC with the reduction of 50%, which suggests qualitatively a tough or ductile state of the tungsten. These observations indicate that the ductility of tungsten can be improved through MDC processing.

Recent investigations show that the DBTT of commercial purity tungsten decreases monotonically with the strain during the plastic working [21]. On one hand, the grain refinement generated by MDC leads to an increase of grain boundaries and a decrease of the impurities concentrated at grain boundaries, which weakens the negative effect of impurities on the brittleness of tungsten. On the other hand, it is difficult for the generation and broadening of cracks on the materials with refined grain and then the fine-grained material is of high toughness.

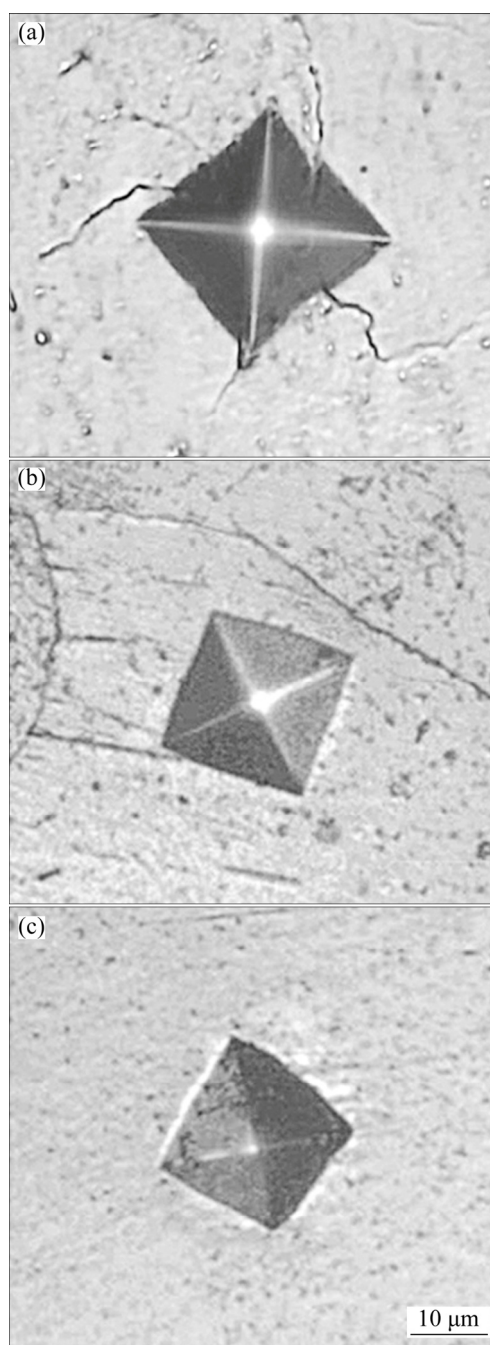


Fig. 7 Morphologies of microhardness indentations: (a) Initial sintered tungsten; (b) MDC-processed tungsten with reduction of 30%; (c) MDC-processed tungsten with reduction of 50%

3.4 Recrystallization behavior

The stability of the microstructures processed by SPD is of significance in the view of practical applicability. Therefore, it is essential to analyze the recrystallization behavior of MDC-processed tungsten samples.

Accordingly, the recrystallization temperature for the commercial pure tungsten is in the range from 1473 to 1673 K and the value is influenced by several factors, including initial grain size, impurity content, plastic

strain and crystallographic texture. Generally, recrystallization brittleness occurs in tungsten material over the temperature of recrystallization because of the generation and growth of equiaxed recrystallized grains, as well as the segregation of impurity elements around the grain boundaries [4]. To avoid the mechanical properties deterioration of SPD-processed tungsten caused by microstructure transformation from the as-formed fine grains to coarse grains above recrystallization temperature, it is essential to analyze the influence of SPD processing on thermal stability at elevated temperature.

The complete DSC curves obtained for the initial sintered tungsten and the samples processed by MDC with the reduction of 50% are plotted in Fig. 8. It can be seen that the DSC graphs of the sintered tungsten and processed tungsten with 50% reduction are obviously different. For the sintered tungsten with a lot of microscopic pores, endothermic reaction leads to the heat flow decreasing during heating.

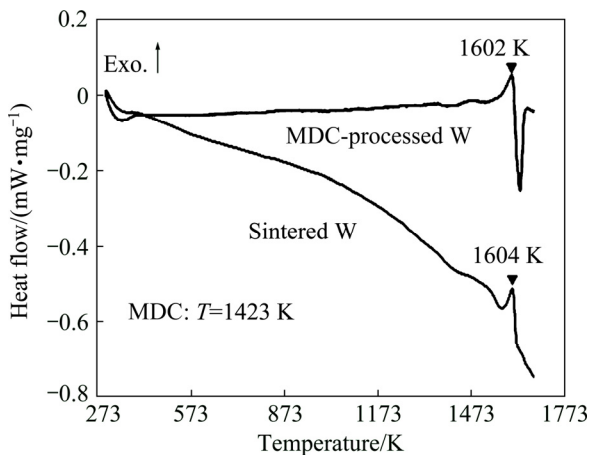


Fig. 8 DSC curves of sintered and MDC-processed tungsten

According to theory of differential scanning calorimetry, a single exothermic peak detected during DSC scanning is associated with recovery and recrystallization. The DSC response is connected to the recrystallization kinetics by the peak temperature, which is the temperature at which 50% recrystallization has occurred [22]. Generally, the recrystallization temperature is considered to be approximately equal to the temperature when the recrystallization fraction is up to 50% [23]. Therefore, it can be detected from Fig. 8 that the recrystallization for the initial sintered tungsten occurs at about 1604 K and the value remains approximately constant (about 1602 K) for the sample processed by MDC with the reduction of 50%.

Based on the traditional theory for polycrystalline materials processed by plastic deformation, higher dislocation density in the sample indicates more strain-stored energy and provides a larger driving force

for recovery and recrystallization, which results in the shift of exothermic peak towards the lower temperature direction during DSC measurement. The strain-stored energy supported by the dislocation density (calculated from XRD) can be determined as

$$E_d = \frac{1}{2} \rho G b^2 \quad (4)$$

where G is shear modulus and the value is 161 GPa for commercial pure tungsten, b is the absolute value of Burgers vector and ρ is the dislocation density.

Therefore, the strain-stored energy of the initial sintered tungsten is 0.09978 J/g, and the value experiences a significant increase and reaches 0.25389 J/g for the sample processed by MDC with the reduction of 50%. The values of strain-stored energy for each sample are in consistence with those obtained by calculating the area under the exothermic peak of each DSC curve, which are 0.28878 and 0.391252 J/g, respectively. It should be noted that the strain-stored energy based on Eq. (4) is lower than the stored energy calculated from DSC curve for each sample, which is due to the fact that several factors have effect on the stored energy except for the strain-stored energy, such as subgrain orientation, shear rate, boundary energy and subgrain size [24].

From the DSC thermogram, it can be seen that the recrystallization temperature for the sample processed by MDC is nearly unchanged compared with that for the initial sintered tungsten, which indicates that the dependence of recrystallization temperature on deformation degree is weak for MDC processing. In other words, the microstructures with higher stored energy developed through MDC are of thermal stability. It is contrary to the widespread conception that recrystallization temperature decreases with the induced strain during conventional plastic deformation. For the strain-hardened materials produced by conventional plastic deformation, the local high dislocation density and large strain gradient result in recrystallization by means of nucleation and growth. The recrystallization mechanism for the sample after MDC is similar to that for the conventional plastic deformation, namely static recrystallization (SRX) [25].

The kinetics of recrystallization is governed by the relation:

$$X \propto \dot{N} \dot{G} \quad (5)$$

where X is volume fraction of recrystallization, \dot{N} is the rate of nucleation, and \dot{G} is interface migration rate:

$$\dot{G} \propto MP \quad (6)$$

where P is the driving force, and M is the mobility of the recrystallization front.

There are much higher density of nucleation sites in the tungsten sample processed by MDC distributing around the high angle grain boundaries induced by plastic deformation. Therefore, the rate of nucleation (\dot{N}) increases for the MDC-processed tungsten.

In Eq. (6), the mobility (M) is an increasing function of misorientation for low angle boundaries and a constant for high angle boundaries [22]. The average misorientation for low angle boundaries increases from approximately 4.4° for the initial sintered tungsten to 6.8° after one pass of MDC with the reduction of 50%. Therefore, the mobility (M) is likely to increase for MDC sample and the accelerated recrystallization leads to a lower peak temperature. According to the strain-stored energy based on Eq. (4) and the stored energy calculated from DSC curves, the stored energy, namely the driving force (P), increases for the MDC-processed tungsten. Therefore, the increasing values of mobility (M) and driving force (P) make contribution to the increase of interface migration rate (\dot{G}).

It should be noted that inhomogeneities in the microstructure lead to easier recrystallization in any deformed metallic material [26]. The refined grains with similar size in the sample result in the homogeneous distribution of these nucleation sites around the subgrain or grain boundaries, which indicates that it costs more energy to activate all these nucleation sites at the same time. Meanwhile, the enhanced pinning effect of triple junctions and quadruple points as well as vacancy drag-effects occurs in the tungsten sample with refined grains processed by MDC, which results in the increase of recrystallization activation energy after MDC [23]. By considering all the mentioned factors in context, the interface migration rate (\dot{G}) could be decreased for the MDC-processed tungsten. The synergistic effects of the increase of nucleation rate (\dot{N}) and the decrease of interface migration rate (\dot{G}) lead to the approximately constant recrystallization temperature for the tungsten samples with and without MDC processing. In other words, the microstructure of MDC-processed tungsten is of thermal stability.

4 Conclusions

1) With the value of MDC reduction increasing, the crystallite size is refined from 35.2 nm for the initial sintered tungsten to 28.2 nm for the sample processed with the reduction of 50%, and the lattice strain increases from 0.086% to 0.18%. The dislocation density also increases to $8.08 \times 10^{14} \text{ m}^{-2}$, which is approximately 3 times higher than that for the initial sintered tungsten.

2) The microhardness increases with the equivalent strain imposed on the sample and reaches $\text{HV}_{0.2} 521$ for the tungsten sample processed by MDC with the

reduction of 50%. This value is approximately 40% higher than that of the initial sintered tungsten at room temperature. Grain refinement and strain-hardening make the major contribution to the enhancement of microhardness. The MDC is feasible to improve the toughness or ductility of sintered tungsten.

3) The processing of MDC results in an increase of stored energy for sintered tungsten, but there is no obvious change in recrystallization temperature according to the exothermic peaks on DSC curves. This phenomenon indicates that the thermal stability of the microstructures for tungsten samples processed by MDC is improved compared with that of the initial sintered powder.

References

- [1] ROTH J, TSITRONE E, LOARTE A, LOARER T, COUNSELL G, NEU R, PHILIPPS V, BREZINSEK S, LEHNEN M, COAD P, GRISOLIA C, SCHMID K, KRIEGER K, KALLENBACH A, LIPSCHULTZ B, DOERNER R, CAUSEY R, ALIMOV V, SHU W, OGORODNIKOVA O, KIRSCHNER A, FEDERICI G, KUKUSHKIN A. Recent analysis of key plasma wall interactions issues for ITER [J]. *Journal of Nuclear Materials*, 2009, 390–391(1): 1–9.
- [2] RIETH M, DUDAREV S L, VICENTE S M G D, AKTAA J, AHLGREN T, ANTUSCH S, ARMSTRONG D E J, BALDEN M, BALUC N, BARTHE M F. Recent progress in research on tungsten materials for nuclear fusion applications in Europe [J]. *Journal of Nuclear Materials*, 2013, 432(1–3): 482–500.
- [3] GLUDOVATZ B, WURSTER S, HOFFMANN A, PIPPAN R. Fracture toughness of polycrystalline tungsten alloys [J]. *International Journal of Refractory Metals and Hard Materials*, 2010, 28(6): 674–678.
- [4] EKBOM L, ANTONSSON T. Tungsten heavy alloy: Deformation texture and recrystallization of tungsten particles [J]. *International Journal of Refractory Metals and Hard Materials*, 2002, 20(5–6): 375–379.
- [5] KURISHITA H, AMANO Y, KOBAYASHI S, NAKAI K, ARAKAWA H, HIRAOKA Y, TAKIDA T, TAKEBE K, MATSUI H. Development of ultra-fine grained W–TiC and their mechanical properties for fusion applications [J]. *Journal of Nuclear Materials*, 2007, 367–370(Part B): 1453–1457.
- [6] WEI Q, KECSKES L J, RAMESH K T. Effect of low-temperature rolling on the propensity to adiabatic shear banding of commercial purity tungsten [J]. *Materials Science and Engineering A*, 2013, 578: 394–401.
- [7] KIRAN U R, PANCHAL A, SANKARANARAYANA M, NANDY T K. Tensile and impact behavior of swaged tungsten heavy alloys processed by liquid phase sintering [J]. *International Journal of Refractory Metals and Hard Materials*, 2013, 37: 1–11.
- [8] LIU Jin-xu, LI Shui-kui, ZHOU Xiao-qing, WANG Ying-chun, YANG Jia. Dynamic recrystallization in the shear bands of tungsten heavy alloy processed by hot-hydrostatic extrusion and hot torsion [J]. *Rare Metal Materials and Engineering*, 2011, 40(6): 957–960.
- [9] VALIEV R Z, ISLAMGALIEV R K, ALEXANDROV I V. Bulk nanostructured materials from severe plastic deformation [J]. *Progress in Materials Science*, 2000, 45(2): 103–189.
- [10] FALESCHINI M, KREUZER H, KIENER D, PIPPAN R. Fracture toughness investigations of tungsten alloys and SPD tungsten alloys [J]. *Journal of Nuclear Materials*, 2007, 367–370(Part A): 800–805.

- [11] WEI Q, ZHANG H T, SCHUSTER B E, RAMESH K T, VALIEV R Z, KECSKES L J, DOWDING R J, MAGNESS L, CHO K. Microstructure and mechanical properties of super-strong nanocrystalline tungsten processed by high-pressure torsion [J]. *Acta Materialia*, 2006, 54(15): 4079–4089.
- [12] ZHANG Y, GANEEV A V, GAO X, SHARAFUTDINOV A V, WANG J T, ALEXANDROV I V. Influence of HPT deformation temperature on microstructures and thermal stability of ultrafine grained tungsten [J]. *Materials Science Forum*, 2008, 584–586: 1000–1005.
- [13] MATHAUDHU S N, DEROSSET A J, HARTWIG K T, KECSKES L J. Microstructures and recrystallization behavior of severely hot-deformed tungsten [J]. *Materials Science and Engineering A*, 2009, 503(1–2): 28–31.
- [14] TANG Lie-chong, LIU Chu-ming, CHEN Zhi-yong, JI Da-wei, XIAO Hong-chao. Microstructures and tensile properties of Mg–Gd–Y–Zr alloy during multidirectional forging at 773 K [J]. *Materials and Design*, 2013, 50: 587–596.
- [15] ESTRIN Y, VINOGRADOV A. Extreme grain refinement by severe plastic deformation: A wealth of challenging science [J]. *Acta Materialia*, 2013, 61: 782–817.
- [16] GONZÁLEZ G, LARA G A. Characterization of precipitation in Al–Mg–Cu alloys by X-ray diffraction peak broadening analysis [J]. *Materials Characterization*, 2008, 59: 773–780.
- [17] ZHANG Z, ZHOU F, LAVERNIA E J. On the analysis of grain size in bulk nanocrystalline materials via X-ray diffraction [J]. *Metallurgical and Materials Transaction A*, 2003, 34: 1349–1355.
- [18] LI Ping, WANG Xue, XUE Ke-min, TIAN Ye, WU Yu-cheng. Microstructure and recrystallization behavior of pure W powder processed by high-pressure torsion [J]. *International Journal of Refractory Metals and Hard Materials*, 2016, 54: 439–444.
- [19] WANG Xue, LI Ping, XUE Ke-min. An analysis on microstructure and grain size of molybdenum powder material processed by equal channel angular pressing [J]. *Journal of Materials Engineering and Performance*, 2015, 24: 4510–4517.
- [20] ZHAO Y H, LIAO X Z, JIN Z, VALIEV R Z, ZHU Y T. Microstructures and mechanical properties of ultrafine grained 7075 Al alloy processed by ECAP and their evolutions during annealing [J]. *Acta Materialia*, 2004, 52: 4589–4599.
- [21] ZHANG Y, GANEEV A V, WANG J T, LIU J Q, ALEXANDROV I V. Observations on the ductile-to-brittle transition in ultrafine-grained tungsten of commercial purity [J]. *Materials Science and Engineering A*, 2009, 503: 37–40.
- [22] GU C F, DAVIES C H J. Thermal stability of ultrafine-grained copper during high speed micro-extrusion [J]. *Materials Science and Engineering A*, 2010, 527: 1791–1799.
- [23] HAJIZADEH K, ALAMDARI S G, EGHBALI B. Stored energy and recrystallization kinetics of ultrafine grained titanium processed by severe plastic deformation [J]. *Physica B: Condensed Matter*, 2013, 417: 33–38.
- [24] CHOI S H, JIN Y S. Evaluation of stored energy in cold-rolled steels from EBSD data [J]. *Materials Science and Engineering A*, 2004, 371: 149–159.
- [25] SAKAI T, BELYAKOV A, KAIBYSHEV R, MIURA H, JONAS J J. Dynamic and post-dynamic recrystallization under hot, cold and severe plastic deformation conditions [J]. *Progress in Materials Science*, 2014, 60: 130–207.
- [26] IVASISHIN O M, SHEVCHENKO S V, VASILIEV N L, SEMIATIN S L. A 3-D Monte-Carlo (Potts) model for recrystallization and grain growth in polycrystalline materials [J]. *Materials Science and Engineering A*, 2006, 433: 216–232.

多向压缩纯钨烧结体的组织及热稳定性

李萍, 孙大智, 王雪, 薛克敏, 华睿, 吴玉程

合肥工业大学 材料科学与工程学院, 合肥 230009

摘要: 对纯度为 99.9% 的纯钨烧结体在 1423 K 进行不同压下量的多向压缩(MDC)实验, 采用 X 射线衍射(XRD)、电子背散射衍射(EBSD)及差示扫描量热法(DSC)研究多向压缩前后纯钨试样组织、显微硬度及热稳定性的变化。结果表明, 多向压缩后纯钨烧结体位错密度显著增大, 压下量 50% 纯钨试样的位错密度由初始烧结钨的 3.08×10^{14} 增大至 $8.08 \times 10^{14} \text{ m}^{-2}$, 平均晶粒尺寸由 $83.8 \mu\text{m}$ 细化至 $14.7 \mu\text{m}$, 而显微硬度则由 $\text{HV}_{0.2} 417$ 增大至 $\text{HV}_{0.2} 521$ 。多向压缩后纯钨试样的再结晶温度约为 1600 K, 近似为常数。纯钨烧结体经多向压缩后由于晶粒尺寸减小以及均匀分布的形核点增多, 组织热稳定性得到提高。

关键词: 多向压缩(MDC); 纯钨烧结体; 位错密度; 力学性能; 热稳定性

(Edited by Bing YANG)